



Published in final edited form as:

ACS Med Chem Lett. 2013 April 11; 4(4): 397–401. doi:10.1021/ml300472n.

Discovery and Preliminary SAR of Arylpiperazines as Novel, Brainpenetrant Antiprion Compounds

Zhe Li^{†,‡,§}, Joel Gever^{†,‡}, Satish Rao^{†,‡}, Kartika Widjaja[†], Stanley B. Prusiner^{†,‡,*}, and B. Michael Silber^{†,‡,||}

[†]Institute for Neurodegenerative Diseases, University of California, San Francisco, California

[‡]Department of Neurology, University of California, San Francisco, California

^{||}Department of Bioengineering and Therapeutic Sciences, University of California, San Francisco, California

Abstract

Prion diseases are a group of fatal neurodegenerative disorders that include Creutzfeldt-Jakob disease (CJD) and kuru in humans, BSE in cattle, and scrapie in sheep. Such illnesses are caused by the conversion and accumulation of a misfolded pathogenic isoform (termed PrP^{Sc}) of a normally benign, host cellular protein, denoted PrP^C. We employed high-throughput screening (HTS) ELISAs to evaluate compounds for their ability to reduce the level of PrP^{Sc} in Rocky Mountain Laboratory (RML) prion-infected mouse neuroblastoma cells (ScN2a-cl3). Arylpiperazines were among the active compounds identified but the initial hits suffered from low potency and poor drug-likeness. The best of those hits, such as **1**, **7**, **13**, and **19**, displayed moderate antiprion activity with EC₅₀ values in the micromolar range. Key analogs were designed and synthesized based on the SAR, with analogs **41**, **44**, **46**, and **47** found to have sub-micromolar potency. Analogs **41** and **44** were able to penetrate the blood-brain barrier (BBB) and achieved excellent drug concentrations in the brains of mice after oral dosing. These compounds represent good starting points for further lead optimization in our pursuit of potential drug candidates for the treatment of prion diseases.

Keywords

Neurodegenerative diseases; prion disease; Creutzfeldt-Jakob disease; piperazine; arylpiperazine; SAR

Prion diseases are transmissible, rapidly progressive, fatal, and untreatable neurodegenerative disorders that affect both humans and animals.^{1–3} An early key pathogenic event in diseases caused by the prion protein (PrP) is the conversion of the host cellular PrP, denoted PrP^C, into an aberrant disease-causing isoform, PrP^{Sc}, which accumulates in the CNS of the infected host.^{4–6} The exact mechanism for the conversion of PrP^C to PrP^{Sc} remains unknown.

*To whom correspondence should be addressed. Phone: (415) 476-4482; Fax: (415) 476-8386; stanley@ind.ucsf.edu.

§Global Blood Therapeutics, Inc., South San Francisco, CA 94080

||ELMEDTECH, LLC, San Francisco, CA 94123

Supplementary Table 1, experimental procedures, synthetic procedures for all intermediates. This material is available free of charge via the Internet at <http://pubs.acs.org>.

Author Contributions

All authors have given approval to the final version of the manuscript.

Currently, no treatments exist for prion diseases. Several classes of antiprion compounds that target levels of PrP^{Sc} or PrP^C, including approved drugs (for other uses) in humans as well as experimental small molecules, have been reported.^{7, 8} Some FDA-approved drugs, including quinacrine, phenothiazines, and statins, showed antiprion activity in cell culture but demonstrated no *in vivo* efficacy when tested in prion-infected mice.^{9–11}

We have sought a strategy to treat prion disease by lowering the levels of PrP^{Sc} in prion-infected cell models. Reduced PrP^{Sc} levels are correlated with decreased prion infectivity in cultured cells and delayed development of clinical signs. Using HTS, we identified small molecules that lowered the levels of PrP^{Sc} in an RML prion-infected murine neuroblastoma cell line (ScN2a-cl3)¹², among which were the arylpiperazines (Silber et al., in preparation). Herein, we report SAR analysis and preliminary lead optimization to improve the potency and drug-likeness of the arylpiperazines, and describe the discovery of potent, metabolically stable, BBB-penetrant leads from this series. These compounds are excellent starting points for further lead optimization, with the goal of identifying candidates for further testing in scrapie- and CJD-infected animal models of prion disease.

From our HTS screening efforts of 53,000 compounds, we identified 881 arylpiperazine analogs, 108 of which reduced PrP^{Sc} levels in ScN2a-cl3 cells by ~30%. Of these 108 actives, 58 were subjected to a confirmatory assay, and 41 of which were confirmed, i.e., reduced the level of PrP^{Sc} by ~30% without affecting cell viability (~30% inhibition). A majority (*n*=29) of these compounds, including the top 22 actives, are derivatives of *N*-aryl piperazine having a *para* methylketone or acetyl group on the phenyl ring (**1**, **7**, **13**, **14**, **18**, and **19**) (Table 1). Compounds bearing other substituents on the *N*-phenyl ring, regardless of electronic-rich (**6**, **12**, **17**, and **22**) or electronic-deficient (**5**, **11**, **16**, and **21**) or their positions on the *N*-phenyl ring (compare **3** and **4**; **9** and **10**; **15** and **16**; **20** and **21**), were found to be inactive under our assay conditions (Table 1). This finding argues for the importance of the 4-acetyl group of the *N*-aryl ring in determining the potency of those compounds. We initially postulated that the oxygen of the acetyl group is involved in a HB with the putative target protein (Figure 1a). Conversely, the substitution requirement on the *N*'-nitrogen of the piperazine is less stringent, and both arylmethylenes and heteroarylmethylenes, including benzyl (**1**), 3-pyridinylmethylene (**7**), 2-furanylmethylene (**19**), and 2-thiophenylmethylene (**13** and **14**), are well tolerated and show similar antiprion activities (Table 1).

In our A-ring SAR exploration, we initially tested the requirement for the 4-acetyl group. Compounds with various substituents including 4-acetyl, chloro, fluoro and methoxy as well as their regioisomers (**11–12**, **23–26**, Supplementary Table 1) were purchased and tested. All six compounds showed ~30% PrP^{Sc} reduction and EC₅₀ values >32 μM; thus, they were considered inactive in our assays.

On the B-ring side, several examples of different (hetero) aryls representing phenyl (**1**), 3-pyridyl (**7**), thiophenyl (**13**), and furanyl (**19**) scaffolds were selected to test the influence of the B-ring on antiprion activity. Compounds **1**, **7**, **13**, and **19** were found to possess only moderate activities, with EC₅₀ values ranging 1.95 μM to 4.62 μM (Table 1). For our lead compounds, we aimed for >10-fold potency compared to those identified in the ScN2a-cl3 cell assay. Thus, we embarked on an SAR effort to improve the antiprion potency of the arylpiperazine series. To ensure the lowering of PrP^{Sc} level was not due to cytotoxicity, cell viability in ScN2a-cl3 cells was also carried out to accompany each EC₅₀ ELISA measurement using the fluorescent probe calcein-AM, as reported previously.¹³

We noted from our early SAR that the hydrogen bond acceptor (HBA) acetyl group is clearly important for antiprion potency of these analogs. We sought to replace it with

alternative functionality that could preserve the HB (hydrogen bond) interaction with the putative target. Initially, we surmised that a five-membered heterocycle, such as a 1,3-oxazole, might be a good first choice as an acetyl isostere. Both nitrogen and oxygen atoms of the oxazole are positioned optimally and are capable of functioning as an HBA. We also synthesized and examined the effect of fused benzoxazole systems for possible increased potency (Figure 1b). While the nitrogen or oxygen of the benzoxazole ring may function as an HBA, the fused phenyl ring may also provide additional binding affinity.

To ensure adequate coverage on the B-ring side, three aryl and heteroaryl rings including 3-pyridine, 2-thiophene, 5-methyl-2-furan were selected for these initial SAR studies. A total of 3 oxazoles (**38–40**) and 3 benzoxazoles (**41–43**) were synthesized (Table 2, Schemes 1 and 2). Almost without exception, we found that arylpiperazine analogs did not affect cell viability in ScN2a-c13 cells (Table 2).

With respect to antiprion potency, the oxazoles **38–40** were found to be only weakly active, with EC₅₀ values > 10 μM, suggesting that a simple replacement of HBA group by an oxazole ring was not sufficient to maintain potency. The additional phenyl ring, as seen in the benzoxazole **41–43** (Table 2), was beneficial to antiprion activity: all three analogs showed EC₅₀ values < 10 μM. The 3-pyridyl analog **41** had an EC₅₀ of 0.25 μM, which was 13-fold more potent than both the furanyl **42** and thiophenyl **43** (Table 2). While we cannot specify the exact reason for such potency gain for **41** over other similar analogs with different B-rings, the pyridyl nitrogen atom in **41** may be situated to establish a second HB with the putative molecular target, contributing to its antiprion activity (Figure 1c).

To evaluate the BBB permeability of **41** and its potential as a CNS drug lead, we administered it in mice using a previously reported pharmacokinetic (PK) protocol.¹⁴ Rather than conducting a full PK profile, we utilized an abbreviated protocol to determine key parameters including C_{max} and AUC, which are important for initial compound selection and prioritization. For initial PK studies, all compounds were administered in a single dose (10 mg/kg) by oral gavage in a formulation containing 20% propylene glycol, 5% ethanol, 5% labrosol, and 70% PEG400. Brain and plasma concentrations were measured at 0.5 h, 2 h, 4 h and 6 h after administration. The C_{max} and the AUC from 0 to 6 h (AUC_{0-6h}) for both brain and plasma were calculated. Compound **41** exhibited an excellent brain concentration (C_{max} = 3.63 μM; Table 3). Its very good brain exposure (AUC_{0-6h} = 14.2 μM*h) was approximately 4-fold higher than its plasma exposure (AUC_{0-6h} = 4.18 μM*h), a desired characteristic in a CNS drug. Compound **41** was better absorbed considering its poor microsomal stability (t_{1/2} = 9.2 min, Table 3).

Encouraged by the *in vitro* antiprion potency and *in vivo* PK profile, we decided to expand the SAR around lead **41**, hoping to identify more potent analogs. On the A-ring side, we synthesized a methylated benzoxazole (**48**, Scheme 2) to probe the size constraints of the A-ring binding pocket. Compound **48** was less potent than **41**, with an EC₅₀ of 1.65 μM, indicating that substitution of benzoxazole with a methyl group (**48**) was not well tolerated (data not shown).

We also examined the effect of hydrophobicity on binding affinity by replacing the benzoxazole ring (**41**) with a more hydrophobic benzothiazole ring (**44**, Scheme 2). The sulfur atom of **44** is not capable of acting as an HBA, a role assumed by the oxygen atom in the benzoxazole **41**; the outcome of this compound may allow us to determine which atom (nitrogen or oxygen) in **41** is involved in the HB with the putative target. Replacing the oxygen atom in **41** with a sulfur atom (**44**) had little impact on antiprion activity: **44** was slightly less potent than **41**, with an EC₅₀ = 0.38 μM (Table 2). Presumably, **44** still maintains a HB with the putative target via the nitrogen atom of the benzothiazole ring.

On the B-ring side, we believe the nitrogen atom of **41** is involved as an HBA with the putative target. Addition of a substituent next to the nitrogen may perturb this interaction and thus influence the potency of these analogs. Additionally, because the nitrogen in the pyridine ring is often a target for cytochrome P450 (CYP450) enzymes, the introduction of an adjacent group, in addition to modulating the HB potential and its potency, may also improve the metabolic stability of these pyridine analogs. Therefore, we designed and synthesized several analogs with substituents (**45–47**) next to the nitrogen atom of the pyridine ring (Scheme 2).

The 4-methyl analog **45** was found to be inactive, with an EC₅₀ value >10 μM (Table 2); the B-ring binding pocket should be wide enough to accommodate a small methyl group based on early SAR derived from phenyl, thiophene, and furan analogs. As a result, the loss of antiprion potency of **45** may be due to interference of HB formation between the adjacent nitrogen and its target. In contrast, both 4-F and 4-MeO analogs (**46** and **47**) were active, with EC₅₀ values of 0.38 μM and 1.11 μM, respectively (Table 2). The 4-fluoropyridine analog **46** was 1.5-fold less potent compared to its parent pyridine analog **41**. This observation might be explained by a reduction in the HB strength between nitrogen and the putative target; the neighboring fluoro atom reduces the electron density on the nitrogen atom and thus weakens the strength of the HB. The 4-MeO analog **47** was 4.5-fold less potent than **41**. The bigger methoxy group may hinder and decrease the HB-forming ability or strength of the nitrogen with the target.

Next, we tested the metabolic stability of compounds **44**, **46**, and **47** in mouse and human microsomes (Table 3). Compared to the benzoxazole **41**, the benzothiazole **44** had approximately 2-fold improvement ($t_{1/2}$ = 17.3 min and 9.2 min for **44** and **41**, respectively) in mouse microsomes but was less stable in human microsomes ($t_{1/2}$ = 34.3 min and 50.2 min for **44** and **41**, respectively). The 4-fluoro analog **46** was less stable in both mouse and human microsomes compared to **41**. The fluorine atom could affect the oxidation of pyridine ring but it also increases the overall hydrophilicity (ChemDraw calculated logP values of 3.86 and 4.09 for **41** and **46**, respectively) of the molecule and may open the possibility of oxidation on other parts of the molecule. The methoxy analog **47** had an approximately 3-fold increase in stability in both human and mouse microsomes.

We then profiled compounds **44**, **46**, and **47** in *in vivo* PK studies as described above, focusing on their BBB permeability and brain exposure (Table 3). Both B-ring analogs **46** and **47** had poor exposure in brain and plasma compared to their parent pyridine analog **41**. The benzothiazole analog **44**, however, displayed a favorable PK profile compared to **41**, with a 5-fold brain-to-plasma exposure ratio.

In summary, the initial arylpiperazine HTS hits with low micromolar activity (2.94 μM for **7**) were optimized to yield several leads with >10-fold antiprion potency improvement. The acetyl group in the original HTS hits was replaced with the more drug-like benzoxazole ring. These efforts culminated with the identification of **41** and **44**, both demonstrating robust antiprion potency, favorable PK properties, and good CNS penetration. Further evaluation of these compounds in RML- and CJD-infected animal models is underway.

Supplementary Material

Refer to Web version on PubMed Central for supplementary material.

Acknowledgments

Funding Sources

This work was funded by grants from the NIH (AG021601, AG031220, AG002132, AG10470) and by gifts from the Sherman Fairchild Foundation, Larry F. Hillblom Foundation, Mike Homer Foundation, Lincy Foundation and Robert Galvin.

The authors thank Mr. Phillip Benner for preparing animal dosing and collecting samples in PK studies; Dr. Kurt Giles and the staff of the Hunter's Point animal facility for animal studies; Drs. John Nuss and Robert Wilhelm for reviewing the manuscript.

ABBREVIATIONS

BBB	blood-brain barrier
BINAP	2,2'-bis(diphenylphosphino)-1,1'-binaphthyl
CJD	Creutzfeldt- Jakob disease
DBA	dibenzylideneacetone
DCM	dichloromethane
EC₅₀	half-maximal effective concentration
HBA	hydrogen bond acceptor
HBD	hydrogen bond donor
HTS	high-throughput screening
Pd₂(dba)₃	Tris(dibenzylideneacetone)dipalladium(0)
PrP^C	the normal cellular isoform of the prion protein
PrP^{Sc}	the pathogenic isoform of the prion protein
RML	Rocky Mountain Laboratory
SAR	structure-activity relationship
TEMPO	(2,2,6,6- Tetramethylpiperidin-1-yl)oxyl, or (2,2,6,6- tetramethylpiperidin-1-yl)oxidanyl
TFA	trifluoroacetic acid

References

- Collinge J. Molecular neurology of prion disease. *J Neurol Neurosurg Psychiatry*. 2005; 76:906–919. [PubMed: 15965195]
- Aguzzi A, Sigurdson C, Heikenwaelder M. Molecular mechanisms of prion pathogenesis. *Annu Rev Pathol*. 2008; 3:11–40. [PubMed: 18233951]
- Prusiner SB. A unifying role for prions in neurodegenerative diseases. *Science*. 2012; 336:1511–1513. [PubMed: 22723400]
- De Gioia L, Selvaggini C, Ghibaudi E, Diomede L, Bugiani O, Forloni G, Tagliavini F, Salmona M. Conformational polymorphism of the amyloidogenic and neurotoxic peptide homologous to residues 106–126 of the prion protein. *J Biol Chem*. 1994; 269:7859–7862. [PubMed: 7907586]
- Hegde RS, Tremblay P, Groth D, Prusiner SB, Lingappa VR. Transmissible and genetic prion diseases share a common pathway of neurodegeneration. *Nature*. 1999; 402:822–826. [PubMed: 10617204]
- Legname, G.; DeArmond, SJ.; Cohen, FE.; Prusiner, SB. Pathogenesis of prion diseases. In: Uversky, VN.; Fink, AL., editors. *Protein Misfolding, Aggregation, and Conformational Diseases*. Springer; New York: 2007. p. 125-146.
- Trevitt CR, Collinge J. A systematic review of prion therapeutics in experimental models. *Brain*. 2006; 129:2241–2265. [PubMed: 16816391]

8. Weissmann C, Aguzzi A. Approaches to therapy of prion diseases. *Annu Rev Med.* 2005; 56:321–344. [PubMed: 15660515]
9. Collins SJ, Lewis V, Brazier M, Hill AF, Fletcher A, Masters CL. Quinacrine does not prolong survival in a murine Creutzfeldt-Jakob disease model. *Ann Neurol.* 2002; 52:503–506. [PubMed: 12325081]
10. Barret A, Tagliavini F, Forloni G, Bate C, Salmona M, Colombo L, De Luigi A, Limido L, Suardi S, Rossi G, Auvre F, Adjou KT, Sales N, Williams A, Lasmezas C, Deslys JP. Evaluation of quinacrine treatment for prion diseases. *J Virol.* 2003; 77:8462–8469. [PubMed: 12857915]
11. Nakajima M, Yamada T, Kusuhara T, Furukawa H, Takahashi M, Yamauchi A, Kataoka Y. Results of quinacrine administration to patients with Creutzfeldt-Jakob disease. *Dement Geriatr Cogn Disord.* 2004; 17:158–163. [PubMed: 14739538]
12. Ghaemmaghami S, May BCH, Renslo AR, Prusiner SB. Discovery of 2-aminothiazoles as potent antiprion compounds. *J Virol.* 2010; 84:3408–3412. [PubMed: 20032192]
13. May BCH, Zorn JA, Witkop J, Sherrill J, Wallace AC, Legname G, Prusiner SB, Cohen FE. Structure-activity relationship study of prion inhibition by 2-aminopyridine-3,5-dicarbonitrile-based compounds: Parallel synthesis, bioactivity and in vitro pharmacokinetics. *J Med Chem.* 2007; 50:65–73. [PubMed: 17201410]
14. Gallardo-Godoy A, Gever J, Fife KL, Silber BM, Prusiner SB, Renslo AR. 2-Aminothiazoles as therapeutic leads for prion diseases. *J Med Chem.* 2011; 54:1010–1021. [PubMed: 21247166]

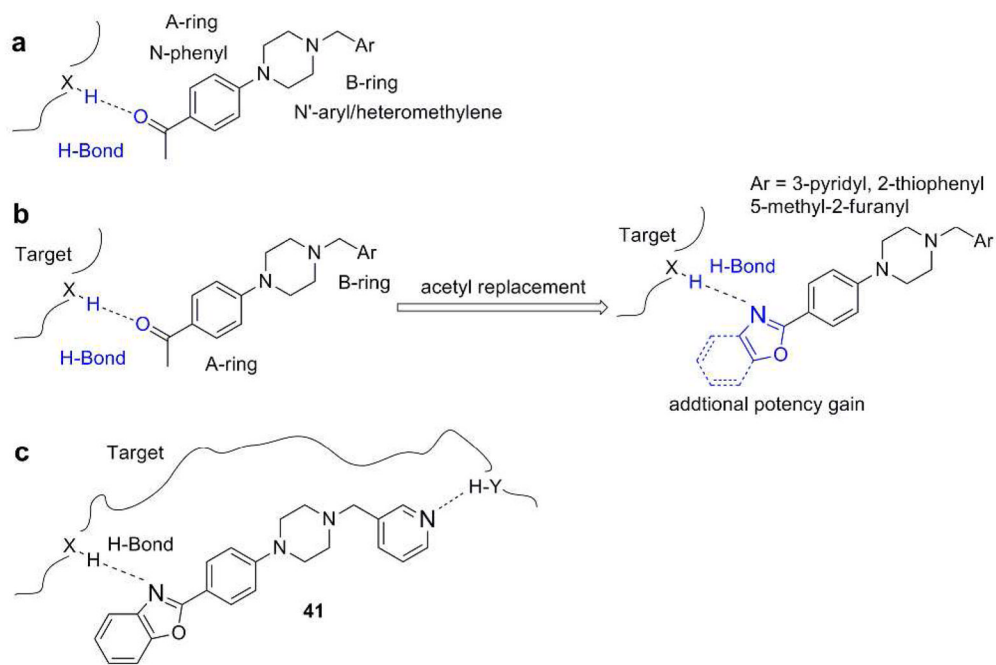
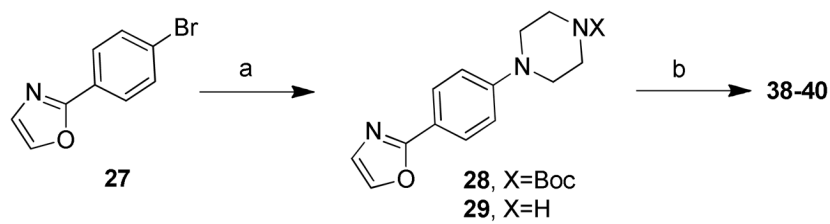
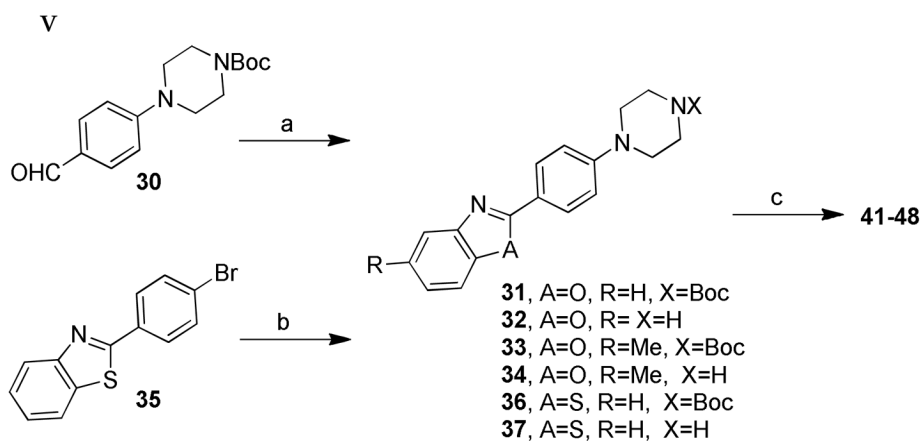


Figure 1.

- (a) Arylpiperazine lead, showing HB interaction between its 4-acetyl group and the putative target. (b) Design of piperazine analogs: replacement of acetyl with oxazole or benzoxazole. (c) Compound **41**, showing its HB interactions with the putative target.

**Scheme 1. Synthesis of oxazole analogs 38–40.^a**

^aReaction conditions: (a) (i) *tert*-butyl piperazinecarboxylate/*t*-BuOK, Pd₂(dba)₃ (5% mmol), BINAP (15% mmol), toluene, reflux, 12 h, 70%; (ii) TFA, DCM, RT, 3 h, 93%; (b) RCHO/HCOOH (2 equiv), anhydrous DMF, 100 °C, 3 h, 21–37%.



Scheme 2. Synthesis of compounds 41–48.^a

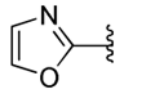
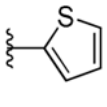
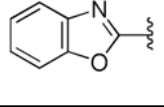
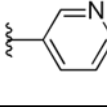
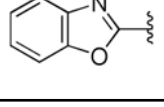
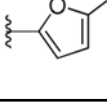
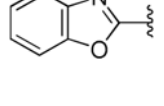
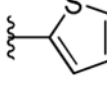
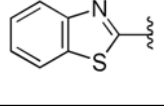
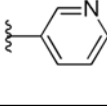
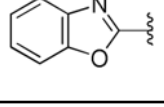
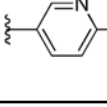
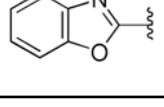
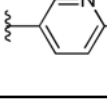
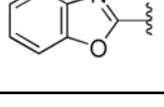
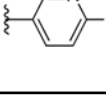
^aReaction conditions: (a) (i) 2-aminophenol or 2-amino-4-methylphenol, O₂, TEMPO, toluene, reflux overnight, 23–81%; (ii) TFA/DCM, RT, 3 h, 66–77%; (b) (i) *tert*-butyl piperazinecarboxylate/*t*BuOK, Pd₂(dba)₃ (5% mmol), BINAP (15% mmol), toluene, reflux, 12 h, 60%; (ii) TFA/DCM, 25 °C, 3 h, 85%; (c) RCHO/HCOOH (2 equiv), anhydrous DMF, 100 °C, 3 h, 6–44%.

Table 1PrP^{Sc} reduction for selected arylpiperazine analogs.

compd	R ₁	X	PrP ^{Sc} reduction (%)
1	4-MeCO-	CH	94
2	H	CH	5
3	3-Cl	CH	7
4	4-Cl	CH	6
5	4-F	CH	7
6	4-MeO	CH	7
7	4-MeCO-	N	73
8	H	N	4
9	3-Cl	N	4
10	4-Cl	N	0
11	4-F	N	27
12	4-MeO	N	10

compd	R ₂	Y	R ₃	PrP ^{Sc} reduction (%)
13	4-MeCO-	S	H	91
14	4-MeCO-	S	4-Me	78
15	3-Cl	S	3-Br	34
16	4-Cl	S	2-Br	12
17	4-MeO	S	H	16
18	4-MeCO-	O	H	96
19	4-MeCO-	O	2-Me	78
20	3-Cl	O	H	6
21	4-Cl	O	H	13
22	4-MeO	O	2-Br	6

Table 2Antiprion potency (EC₅₀) and cell viability (LC₅₀) for selected arylpiperazine analogs.

compd	R ¹	R ²	EC ₅₀ ± SEM (μM) ^a	LC ₅₀ (μM) ^a
38			>10	>10
39			>10	>10
40			>10	>10
41			0.25 ± 0.03	>10
42			3.28 ± 0.49	>10
43			4.17 ± 2.19	>10
44			0.38 ± 0.02	>10
45			>10	>10
46			0.38 ± 0.02	>10
47			1.12 ± 0.58	>10

^aNumber of tests for EC₅₀ and LC₅₀ measurement: 3

Table 3

In vivo PK parameters and *in vitro* microsomal stability for arylpiperazines (single oral dose of 10 mg/kg).

compd	Brain Exposure		Plasma Exposure		Microsomal Stability		
	C _{max} (μM)	AUC (μM*h)	C _{max} (μM)	AUC (μM*h)	t _{1/2} (min)		
41	3.63 ± 0.85	14.20 ± 0.57	0.91 ± 0.11	4.18 ± 0.60	Mo	Hu	50.2
44	3.03 ± 0.53	14.40 ± 0.15	0.60 ± 0.01	2.68 ± 0.39	17.3		34.3
46	0.36 ± 0.06	1.30 ± 0.18	0.40 ± 0.15	1.17 ± 0.09	7.3		43.6
47	1.55 ± 0.78	3.03 ± 1.04	0.65 ± 0.38	1.07 ± 0.47	25.2		>60